Imaging the early stages of phospholipase C/sphingomyelinase activity on vesicles containing coexisting ordered-disordered and gel-fluid domains[S]

Maitane Ibarguren,* David J. López,* L.-Ruth Montes,* Jesús Sot,* Adriana I. Vasil,† Michael L. Vasil,† Félix M. Goñi,* and Alicia Alonso[1,*]

Unidad de Biofísica (Centro Mixto CSIC-UPV/EHU),* y Departamento de Bioquímica, Universidad del País Vasco, Bilbao, Spain; and Department of Microbiology,† School of Medicine, University of Colorado Denver, Aurora, CO

Abstract The binding and early stages of activity of a phospholipase C/sphingomyelinase from *Pseudomonas aeruginosa* on giant unilamellar vesicles (GUV) have been monitored using fluorescence confocal microscopy. Both the lipids and the enzyme were labeled with specific fluorescent markers. GUV consisted of a mixture of phosphatidylcholine, sphingomyelin, phosphatidylethanolamine, and cholesterol in equimolar ratios, to which 5–10 mol% of the enzyme end-product ceramide and/or diacylglycerol were occasionally added. Morphological examination of the GUV in the presence of enzyme reveals that, although the enzyme diffuses rapidly throughout the observation chamber, detectable enzyme binding appears to be a slow, random process, with new bound-enzyme-containing vesicles appearing for several minutes. Enzyme binding to the vesicles appears to be a cooperative process. After the initial cluster of bound enzyme is detected, further binding and catalytic activity follow rapidly. After the activity has started, the enzyme is not released by repeated washing, suggesting a "scooting" mechanism for the hydrolytic activity. The enzyme preferentially binds the more disordered domains, and, in most cases, the catalytic activity causes the disordering of the other domains. Simultaneously, peanut- or figure-eight-shaped vesicles containing two separate lipid domains become spherical. At a further stage of lipid hydrolysis, lipid aggregates are formed and vesicles disintegrate.—Ibarguren, M., D. J. López, L-R. Montes, J. Sot, A. I. Vasil, M. L. Vasil, F. M. Goñi, and A. Alonso. **Imaging the early stages of phospholipase C/sphingomyelinase activity on vesicles containing coexisting ordered-disordered and gel-fluid domains. *J. Lipid Res.* 2011.** 52: **635–645.**

Supplementary key words ceramides • cholesterol • diacylglycerol • fluorescence microscopy • lipid rafts • membranes/physical chemistry • sphingolipids

Phospholipases are essential enzymes in maintaining membrane homeostasis and in the generation of metabolic signals. They are also powerful tools that bacteria use to infect and eventually destroy eukaryotic cells by helping in the degradation of the target cell membranes. Phospholipase C (PLC) enzymes cleave the phosphodiester bond between the diacylglycerol moiety and the phosphoryl base (phosphorylcholine, phosphorylethanolamine, and others), characteristic of each phospholipid class. Most sphingomyelinases hydrolyze the equivalent bond between ceramide (Cer) and phosphorylcholine in sphingomyelin (SM). From the point of view of their enzyme activities, phospholipases and lipases in general are rather unique among enzymes in that their substrates and end products do not occur freely in solution but are instead found to make up part of the cell membrane.

Early work from our laboratory (1) had shown that phospholipid hydrolysis catalyzed by PLC from *Bacillus cereus* was able to induce aggregation and fusion of large unilamellar vesicles (LUV). That work was confirmed by other studies (2) and was later extended to other PLCs (3–7). More recently, Montes et al. (8) described the leakage-free membrane fusion induced by the hydrolytic activity of

This work was supported in part by Spanish Ministerio de Ciencia e Innovación Grants BFU 2008-01637/BMC (A.A.) and BFU 2007-62062 (F.M.G.); by Basque Government Grant IT 461-07 (F.M.G.) and ETORTEK 07/26 (A.A.); and by National Institutes of Health Grant HL-062608 (M.L.V.). Its contents are solely the responsibility of the authors and do not necessarily represent the official views of the National Institutes of Health or other granting agencies. M. Ibarguren was a graduate student supported by the Basque Government.

Manuscript received 4 November 2010 and in revised form 10 January 2011.

Published, JLR Papers in Press, January 20, 2011
DOI 10.1194/jlr.M012591

Abbreviations: Cer, ceramide; Chol, cholesterol; DAG, diacylglycerol; DiI, dioctadecyl-3,3,3′3′-tetramethylindocarbocyanine perchlorate; NPPC, *p*-nitrophenylphosphatidylcholine; PC, phosphatidylcholine; PE, phosphatidylethanolamine; PLA_2, phospholipase A_2; PLC, phospholipase C.

[1] To whom correspondence should be addressed.
e-mail: alicia.alonso@ehu.es

[S] The online version of this article (available at http://www.jlr.org) contains supplementary data in the form of two figures and two videos.

$PlcHR_2$ from *Pseudomonas aeruginosa*. This enzyme is the paradigm member of a novel PLC/phosphatase superfamily, first described in one of our studies (9).

A different line of research, also pertinent to the present work, has underlined the significance of lateral heterogeneity, i.e., the existence of domains in cell membranes (10). Studies of pure lipid vesicles (liposomes) have demonstrated that even with pure lipids or simple two-lipid mixtures, domain formation can occur. The coexistence of gel and fluid (11–13), gel and liquid-ordered (14), and fluid-ordered and fluid-disordered domains (15) has been shown by a variety of physical methods (16–18). Moreover, the advent of giant unilamellar vesicles (GUV) (19, 20) and the application of confocal fluorescence microscopy (21, 22) have allowed visualization of domains and domain coexistence in a variety of lipid membranes. In a recent study from one of our laboratories (23), fluorescence confocal microscopy and differential scanning calorimetry were used in combination to study the phase behavior of GUV bilayers composed of phosphatidylcholine, SM, phosphatidylethanolamine, and cholesterol (PC:SM:PE: Chol) in equimolar mixtures, in the presence or absence of 10 mol% egg Cer. In the absence of Cer, separate liquid-ordered and liquid-disordered domains were observed in the vesicles. In the presence of Cer, gel-like domains appeared within the liquid-ordered regions. The morphological and calorimetric data were interpreted in terms of cholesterol displacement by Cer from SM- and Chol-rich liquid-ordered regions. In contrast to Cer, when 10 mol% egg diacylglycerol (DAG) was added to the PC:SM:PE:Chol mixture, homogeneous vesicles consisting only of liquid-disordered bilayers were observed (23). This study confirmed and expanded several related observations from other laboratories (24–26).

The relationship between phospholipase activity and lipid phase behavior remains a field of active research. Several details regarding the kinetics, morphology, and mechanisms of formation of segregated domains by some phospholipases, including sphingomyelinase, have been elucidated using different model membrane systems and mixtures of lipids. The dependence of the activities of phospholipase A_2 (PLA_2), PLC, and sphingomyelinase on the lipid physical state, showing that these enzymes preferably degrade the more fluid phase state, was demonstrated in early studies using lipid monolayers and bilayer vesicles (27–32). Our previous studies of PLC-promoted membrane fusion correlated enzyme activity and the generation of nonlamellar structures that would in turn be fusion intermediates (33). Further results from our laboratory (34) have related the activity of phosphatidylinositol-specific PLC to the degree of molecular order in membranes. Also, Bell and co-workers (35, 36) and Mouritsen and co-workers (37, 38) have explored the relationship between PLA_2 activity and the physical state of the membrane. Holopainen et al. (39) observed lipid microdomain formation that resulted from sphingomyelinase activity on fluid membranes of PC/SM. Contreras et al. (40) reported that bacterial sphingomyelinase activity varied with the physical state of the substrate, increasing in the order gel < liquid-ordered < liquid-disordered. Mechanisms for phospholipase action, including domain formation by sphingomyelinase, have been reported recently (41–43). Also, the dependence of sphingomyelinase activity on the membrane physical properties has been stressed in a recent report (44). GUVs have been used in connection with the study of lipases (45, 46). In particular, Holopainen et al. (47) described the vectorial budding of vesicles by asymmetrical enzymatic formation of Cer in giant liposomes. Equally relevant in this context are the studies by Holopainen et al. (48) and López-Montero et al. (49), in which lipases were added in situ to single GUVs, and various effects, e.g., vesicle shrinking or generation of surface tension, were observed.

The present contribution is intended to provide a link between the bulk (in cuvette) studies of lipase activity on lipid bilayers in different physical states (27–44) and the morphological data obtained largely with GUV of homogenous lipid compositions (45–49). This work is based on our previous studies of phase separation in GUVs (23) as well as our experience with $PlcHR_2$ (8, 50). A detailed description of the binding and activity of $PlcHR_2$ on GUV exhibiting gel/fluid and fluid-ordered/fluid-disordered domain coexistence is offered, and mechanistic aspects of $PlcHR_2$ activity are discussed.

MATERIALS AND METHODS

Materials

$PlcHR_2$ was purified as previously described (9). Egg PC, egg PE, and egg DAG were purchased from Lipid Products (South Nutfield, UK). Egg SM, egg Cer, and Chol were from Avanti Polar Lipids (Alabaster, AL). The compound 1,1′-dioctadecyl-3,3,3′3′-tetramethylindocarbocyanine perchlorate (DiI) and an Alexa Fluor 633 protein labeling kit were from Invitrogen (Eugene, OR).

Construction and purification of $PlcHR_2$ T178A

The Thr178Ala mutant PlcH was identified based on an alanine scanning mutagenesis experiment to identify enzymatically deficient mutants. A 1,000 bp region of the plcH gene was mutagenized, and the pooled mutated DNA was used to replace the corresponding wild-type plcH gene in an *Escherichia coli* plasmid (51). Individual clones carrying the mutated plcH gene were then screened for PLC activity using the synthetic PLC substrate *p*-nitrophenyl phosphatidylcholine (NPPC) (9). Individual clones that expressed either low or no NPPC activity compared with one that had the wild-type plcH gene were fully sequenced to determine the location of the individual mutations. One of these clones that carried the mutation, in which Thr was changed to Ala at position 178, was chosen for further characterization. The plcH gene carrying the Thr178Ala mutation, along with the plcR gene (encoding a chaperone for PlcH secretion), was then cloned into an expression plasmid (pADD3268) with a T7 promoter and transformed into a *P. aeruginosa* strain (pADD1976), which carries a chromosomal isopropyl β-D-1-thiogalactopyranoside-inducible T7 polymerase driven by a lacUV5 promoter (9). This expression system allows the expression and secretion of mutant PlcHR proteins (e.g., Thr178Ala). This mutant was then purified from the culture supernatant as previously described for native PlcHR (9). However, because the Thr178Ala mutant has little or no detectable PLC activity, we tracked its purification using

monoclonal or affinity-purified antibodies against PlcH and PlcR (9). Circular dichroism spectroscopy and thermal denaturation studies revealed there were no significant differences between the structure of the wild-type PlcHR and that of the Thr178Ala mutant (data not shown).

It is noteworthy that Thr178 of PlcH corresponds to Ser175 in a PlcH ortholog (i.e., AcpA), which is expressed by *Francisella tularensis* (52). However, unlike PlcH, AcpA has phosphatase activity but not authentic PLC activity (51). The Ser175 of AcpA was identified in the active site of AcpA, which is only defined based on the crystal structure of AcpA in context of the interactions of 10 amino acids, including Ser175, with vanadate (a phosphate analog), which provides a model for the phosphate moiety of a phosphomonoester or phosphodiester bond of an AcpA or PLC substrate (52).

GUV preparation and fluorescence microscopy

GUVs were prepared using the electroformation method developed by Angelova et al. (19), using a specialized chamber supplied by L. A. Bagatolli (Odense, Denmark) that allows direct visualization under the microscope (53). Stock solutions of lipids (0.2 mg/ml total lipid containing 0.2 mol% DiI) were prepared in a chloroform-methanol (9:1, v/v) solution. Three microliters of the appropriate stocks were added to the surface of Pt electrodes, and solvent traces were removed by evacuating the chamber under high vacuum for at least 2 h. Then, the Pt electrodes were covered with 400 µl of 10 mM HEPES (pH 7.4), previously heated to 60°C. The Pt wires were connected to an electric wave generator (TG330 function generator; Thurlby Thandar Instruments, Huntington, UK) under AC field conditions (frequency, 10 Hz; amplitude, 1 V) for 2 h at 60°C. After GUV formation, the chamber was placed on an inverted confocal fluorescence microscope (D-Eclipse C1 model; Nikon Inc., Melville, NY). The excitation wavelength for DiI was 561 nm. The images were collected using band-pass filters of 593 ± 20 nm. When required, 2 µl of $PlcHR_2$ labeled with Alexa Fluor 633, at 12 µg/ml, was added to study its effect on the GUVs. In the latter case, an excitation wavelength at 635 nm was used, and images were collected using a long-pass filter of 650 nm. All these experiments were performed at 25–28°C. Image treatment and quantification were performed using EZ-C1 version 3.20 software (Nikon Inc., Melville, NY).

LUV preparation

LUV with diameters of 100–150 nm were prepared by the extrusion method using Nuclepore filters of 0.1 µm pore diameter at room temperature in a solution of 25 mM HEPES, 100 mM NaCl (pH 7.4). Quantitative analysis of the lipid composition of our LUV preparations, as described by Ruiz-Argüello et al. (54), showed that it did not differ significantly from the initial lipid mixture. All experiments were performed at 28°C. Lipid concentration was 0.3 mM, and $PlcHR_2$ was used at 0.5 µg/ml.

TABLE 1. Hydrolytic activity of PlcHR2 on large unilamellar vesicles

Lipid composition	Average enzyme maximum rate ± SD (nmol/min)	Average % values of hydrolysis ± SD	
		After 5 min	After 10 min
Control	3.1 ± 0.23	15.6 ± 5.25	33.1 ± 3.22
With 10 % Cer	2.6 ± 0.28	16.5 ± 3.50	31.0 ± 5.90
With 10 % DAG	4.1 ± 0.53*	14.8 ± 2.02	37.8 ± 1.35
With 5 mol% DAG plus 5 mol% Cer	5.1 ± 0.36**	29.3 ± 8.60*	52.8 ± 11.00*

Table shows hydrolytic activity of $PlcHR_2$ on large unilamellar vesicles at 28°C. Vesicle composition was PC:SM:PE:Chol (1:1:1:1, molar ratio) with or without DAG or Cer. Data are average values ± standard deviation (SD) (n = 3).

* $P < 0.05$, compared to control (Student's *t*-test).

** $P < 0.001$, compared to control (Student's *t*-test).

Protein labeling

An Alexa Fluor 633 protein labeling kit from Molecular Probes, Inc. (Eugene, OR) was used. This kit labels primary amino groups. The concentration of labeled protein was 60 µg/ml, and each mole of protein contained 4 M dye. Alexa Fluor 633 dye-labeled proteins have fluorescence emission maxima of approximately 632 nm and 647 nm.

Enzyme activity

$PlcHR_2$ activity was assayed by determining water-soluble phosphorus. Liposome concentration was 0.3 mM in all experiments. The enzyme was assayed at 28°C in a solution of 25 mM HEPES, 100 mM NaCl (pH 7.4). Enzyme concentration was 0.5 µg/ml. Aliquots (50 µl) were removed from the reaction mixture at regular intervals and extracted with 250 µl of a chloroform-methanol-hydrochloric acid mixture (200:100:1, v/v/v), and the aqueous phase was assayed for phosphorus.

Statistics

Unless otherwise indicated, data are average values of at least three independent measurements ± 1 standard deviation. Student's *t*-test was used in order to assess the significance of observed differences.

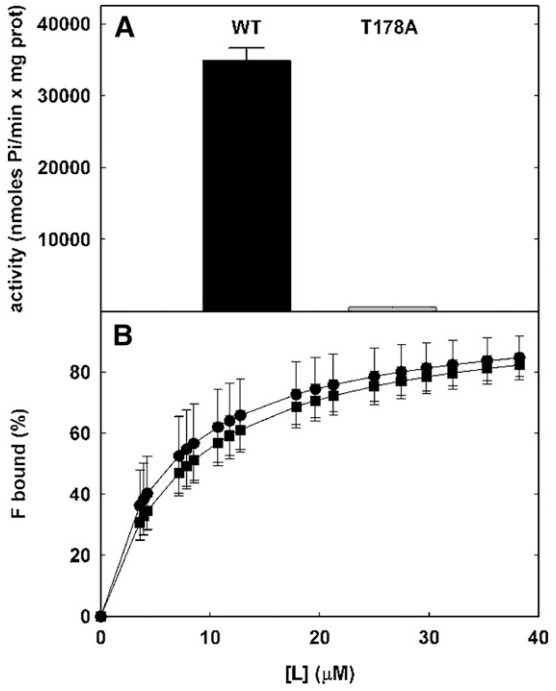

Fig. 1. Phospholipase activity (A) and liposome binding (B) of wild-type (WT) and T178A mutant $PlcHR_2$ are shown. A: Wild-type or mutant PlcHR2 (0.5 µg/ml) was assayed at 37°C on 0.3 mM LUV composed of PC:SM:PE:Chol (1:1:1:1, molar ratio). Phospholipase activity was measured as water-soluble lipid phosphorus. B: Binding of wild-type or mutant PlcHR2 was assayed as an increase in the enzyme's intrinsic fluorescence (F bound) in the presence of increasing concentrations of LUV of the composition indicated above. Data are average values ± SD (n = 3).

RESULTS AND DISCUSSION

Enzyme activity on LUV

The hydrolytic activity of PlcHR2 was assayed on LUV composed basically of PC:SM:PE:Chol (1:1:1:1, molar ratio) at 28°C, the temperature at which confocal microscopy observations were performed. This mixture was used because it contains the main lipids found in mammalian plasma cell membranes and because it was well characterized from previous studies (8, 23). The basic lipid composition was varied, including either 10 mol% Cer, 10 mol% DAG, or 5 mol% Cer plus 5 mol% DAG, to test the effect of enzyme end products in the bilayer. The results can be seen in **Table 1**. The initial rate of hydrolysis for the basic lipid mixture was 3.1 ± 0.23 nmol/min. Initial rates are only slightly, albeit significantly, influenced by lipid composition. The presence of egg DAG with and without Cer causes a small increase in enzyme rate, presumably because of the overall fluidifying effect of DAG and/or due to its tendency to favor negative membrane curvature (23, 33). At 5 min after enzyme addition, about 15% of the PC plus SM solution was hydrolyzed in all mixtures, except the one containing DAG plus Cer, in which 29% hydrolysis was found. At 10 min after $PlcHR_2$ addition, the corresponding values were approximately 33% and 53%, respectively. The 5 and 10 min times were selected for quantitating the extent of lipid hydrolysis because they mark the end of two different periods in the evolution of vesicle morphology (see below).

Hydrolytically inactive T178A mutant

A $PlcHR_2$ mutant was generated in which Thr178 was changed into an Ala residue. This mutation led to a complete loss of phospholipase activity (**Fig. 1A**). The $PlcHR_2$ T178A mutant was also unable to induce vesicle aggregation or release intravesicular aqueous contents (55), while the native enzyme did exhibit those properties (8, 50). However, the T178A mutant's ability to bind LUV composed of PC:SM:PE:Chol (1:1:1:1, molar ratio) was undistinguishable from that of the wild type (Fig. 1B), according to measurements in which the intrinsic enzyme fluorescence was titrated with increasing concentrations of lipid.

Imaging $PlcHR_2$ binding to GUV

The use of GUV allows the direct observation of vesicle and domain morphology and the enzyme effects thereupon. $PlcHR_2$ has been added to preformed GUVs under confocal fluorescence microscopy, and the subsequent morphological changes have been observed and quantitated. Because of the experimental limitations derived from the vesicle thermal motion, the continuous observation of a single vesicle for a period of minutes, as required in this experiment, was only possible at or below 28°C. Thus, GUV experiments were performed at 26–28°C. Lipids from a natural origin (egg) have been used for GUV preparation, despite the additional complexity that this brings to the system, including the possibilities of interdigitation and fluid–fluid immiscibility (56). However, our choice of lipids was guided by our previous work with

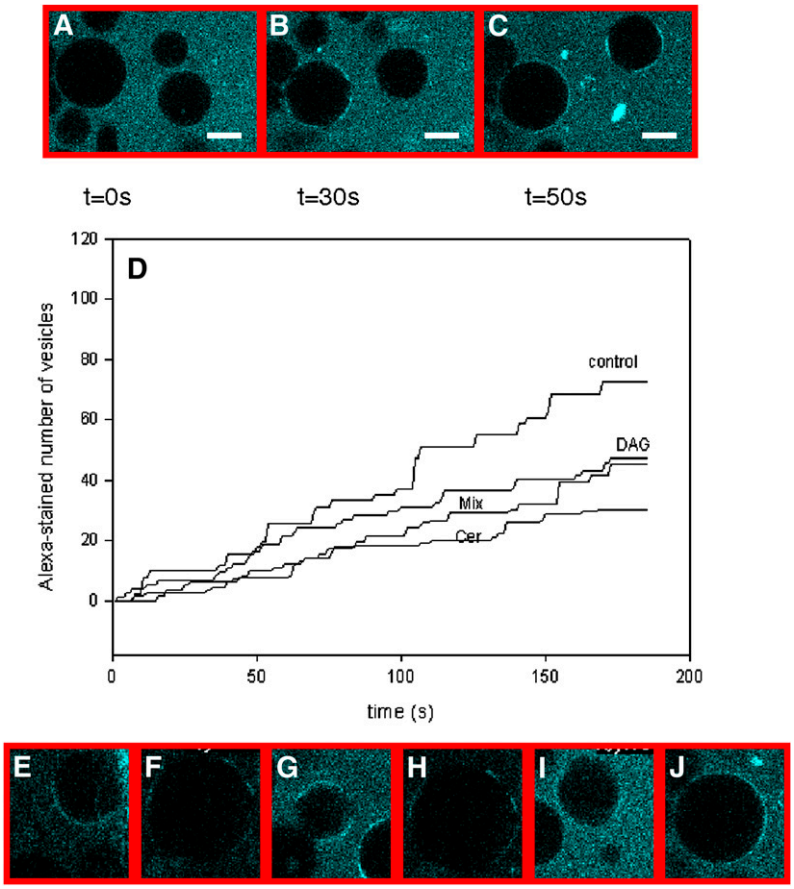

Fig. 2. Images show $PlcHR_2$ binding to GUVs. The enzyme is derivatized with Alexa 633 (pseudocolor blue). Vesicles newly stained with Alexa 633 are shown at different times after enzyme addition. A–C: The gradual binding of enzyme to the same set of vesicles is shown over 50 s (bar = 10 μm). D: A summary of the number of newly stained vesicles is shown as a function of time in 10 videos (10 independent experiments for each lipid composition). Mixture (Mix) = 5 mol% DAG plus 5mol% Cer. E–J: A gallery of newly stained vesicles is shown at the time they were first detected.

phase characterization in an identical system (22) and by the various important early (30, 32, 57) and contemporary (42, 49, 58–60) studies of lipases and lipid domains that have been carried out using natural lipids. GUV are examined individually in most cases, without contact with other vesicles and under reduced mobility conditions; thus, vesicle aggregation or fusion cannot be observed under those conditions. Our methodology is somewhat similar and could be complementary to the one based on supported "membrane islands," as proposed by Simonsen et al. (41).

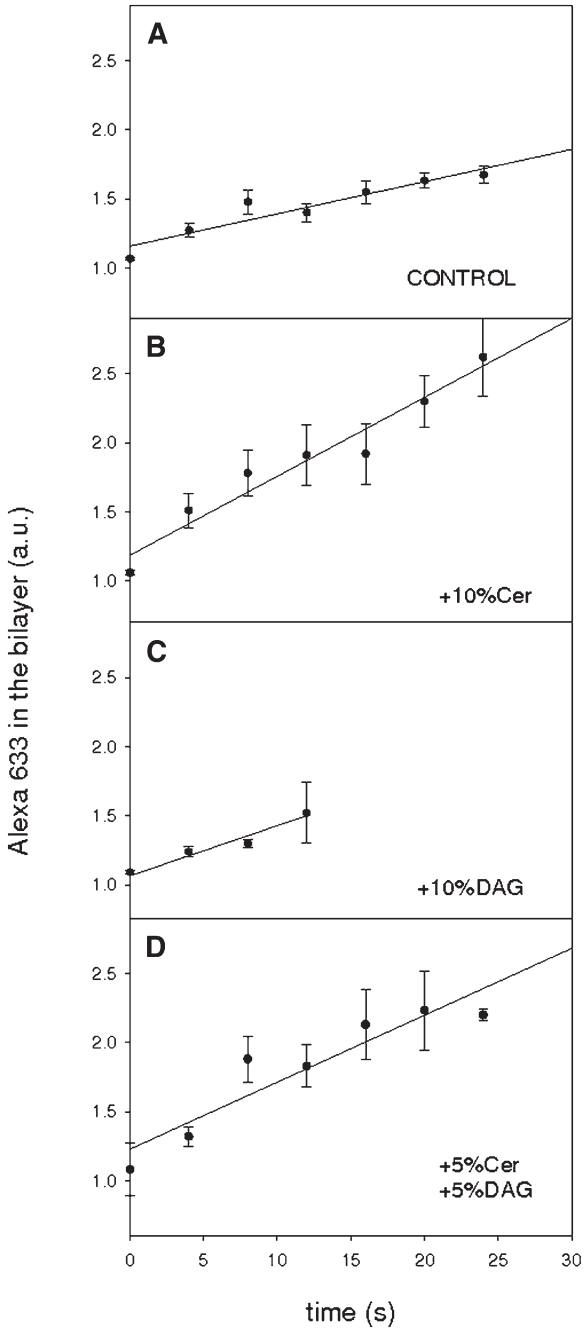

Fig. 3. Progressive $PlcHR_2$ binding to GUVs after initial binding detection. Experimental conditions are as described in the legend to Fig. 1. Enzyme binding is measured as an increase in membrane-bound Alexa fluorescence as a function of time. Time 0 is the moment at which enzyme binding was first detected. A: control; (B) with 10 mol% DAG; (C) with 10 mol% Cer; (D) with 5 mol% Cer plus 5 mol% DAG. Results are average values of 10 vesicles ± SEM.

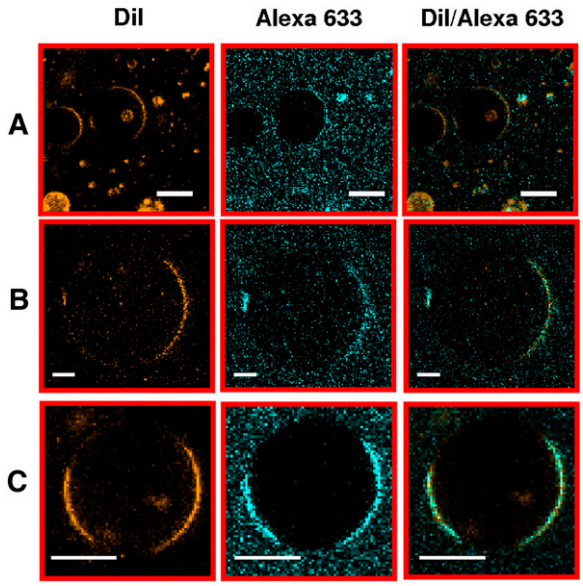

Fig. 4. $PlcHR_2$ preferentially binds to the more disordered domains. Lipid composition: (A) control; (B) with 10 mol% Cer; (C) with 5 mol% Cer plus 5 mol% DAG. Lipids are stained with DiI (yellow). The enzyme was derivatized with Alexa 633 (pseudocolor blue). The column at right shows the merging of DiI and Alexa 633 images. Bar = 10 μm.

$PlcHR_2$ was labeled with Alexa 633 in order to visualize its binding and localization in the vesicle bilayer. Control experiments had shown that Alexa derivatization had not altered the enzyme-specific activity. Adding the Alexa-stained enzyme to the GUV chamber causes the instantaneous appearance of a uniform bright background against which the vesicles are seen as dark objects (**Fig. 2A**). This shows that the enzyme diffuses freely and uniformly in the medium, under our experimental conditions, in a very short time (<10 s) and that it does not penetrate into GUV. Afterward, the accumulation of bright spots on the vesicle surface indicates enzyme absorbance/binding. Interestingly, enzyme binding does not occur with all vesicles simultaneously but is, rather, a random process that extends over minutes. Figure 2B and C shows two stages separated by 30 and 50 s of enzyme binding to the vesicles in the frame seen in Fig. 2A. Note that the initial enzyme binding does not occur uniformly along the vesicle surface. Rather, the enzyme appears to be located initially in small areas (Fig. 2E–J) from which binding propagates along larger fractions of the GUV surface.

When a large number of vesicles are observed, in independent experiments, the phenomenon can be shown in a quantitative way, as shown in Fig. 2D, which summarizes the results of about 10 videos (i.e., 10 independent experiments) for each lipid composition. In all cases, the number of new vesicles containing enzyme clusters increases linearly and slowly for several minutes. Control vesicles, i.e., those containing PC:SM:PE:Chol (in equimolar proportions) become stained at a somewhat higher rate than those containing DAG and/or Cer in addition. Note that

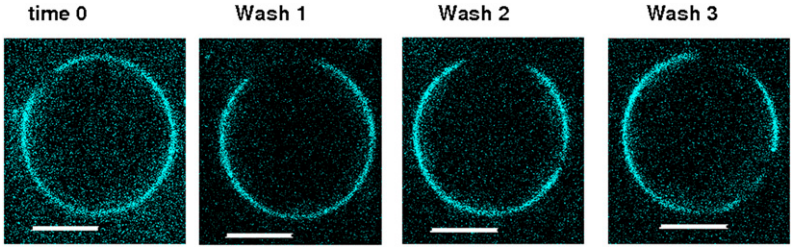

Fig. 5. Effect of repeated washing on the binding of $PlcHR_2$ to GUV is shown. The persistence of bound enzyme after several washing steps is compatible with a processive or "scooting mode" kinetic mechanism of the enzyme.

the data in Fig. 2D correspond to a count of the vesicles that appeared to the observer as newly enzyme bound. Presumably a sizable amount of enzyme molecules must adhere/bind to the GUV bilayer to be detected. It may be that enzyme binding occurs initially in a uniform way and that only after localized cooperative phenomena are the enzyme-enriched membrane regions observed that allow us to detect bound enzyme-containing vesicles. The reason why newly stained vesicles appear over a long time interval is presently unknown. Speculatively, enzyme binding would be favored by thermal instabilities occurring at random in the membranes. According to the data shown Fig. 2D, control vesicles bind the enzymes faster than those containing DAG or DAG plus Cer. As described in our previous work (23), macroscopic phase separation (liquid-ordered and liquid-disordered) was observed in control GUV but not in those containing DAG or DAG plus Cer. Lipid phase separation may offer, at the phase boundary, favorable conditions for instabilities and enzyme binding. Also, as shown in Fig. 2D, GUV containing Cer are seen to be slow enzyme binders. In this case, the Cer-rich rigid domains described previously (23) may display low affinity for enzyme binding. De Tullio et al. (42), in studies using lipid monolayers containing SM and Cer, have observed that sphingomyelinase is preferably located in the SM-rich, liquid-expanded phase, rather than in the Cer-enriched, liquid-condensed areas. Interestingly, those authors do not find an enrichment in enzyme at the phase boundaries.

The results in Fig. 2 support the hypothesis of a cooperative enzyme binding to the bilayer, which would give rise to enzyme-enriched regions detectable under the microscope. Interestingly, Basañez et al. (61), on the basis of cuvette kinetic measurements of PLC on LUV, suggested that the end of the lag period of this enzyme would be marked by the cooperative binding of enzyme molecules to DAG-enriched spots. The data in Fig. 2 appear to confirm this proposal, thus clarifying a mechanistic aspect that may be common at least to several PLC enzymes, namely the cooperative binding to discrete membrane spots at the start of the "burst" of lipase activity. This lag-burst behavior was observed for PLC in GUV by Holopainen et al. (48).

Once a newly stained vesicle is spotted, the increase in membrane-bound Alexa 633 can be quantitated. The results (**Fig. 3**) show that once started, enzyme binding progresses linearly at least for the first 20 s. Reliable measurements at longer times are precluded by the secondary effects caused by enzyme products, DAG and Cer, and concomitant degradation of PC and SM, which alter the bilayer structure in various ways. Remarkably, GUV containing Cer, which were the slowest to show enzyme binding (Fig. 2D), displayed the highest rate of binding once the first enzyme cluster had been detected (Fig. 3B). This is in agreement with the observation that the formation or presence of Cer in lipid monolayers causes increased enzyme adsorption and faster precatalytic activation (but reduced enzyme activity) in independent, surface-regulated processes (62). A comparison of the data in Figs. 2 and 3 suggests that the initial and subsequent steps of phospholipase binding are different phenomena. For vesicles containing 10% additional DAG (Fig. 3C), enzyme binding cannot be reliably measured beyond 15 s due to fast formation of lipid aggregates, presumably nonlamellar, in the bilayer.

$PlcHR_2$ preferentially binds the more disordered domains

With respect to the distribution of $PlcHR_2$ among the various domains, the enzyme has a preference for the more disordered domains (**Fig. 4**), i.e., those into which DiI partitions preferentially (23). The preferential partition of DiI into the more disordered domains cannot be taken for granted (63). In our study, control experiments using Laurdan staining and two-photon confocal microscopy demonstrated that, indeed, DiI partitions preferentially into the liquid-disordered domains (see supplementary

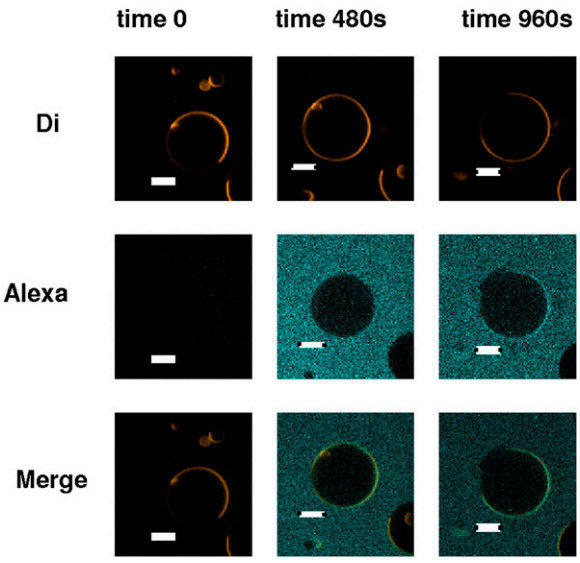

Fig. 6. Binding of the inactive T178A mutant of $PlcHR_2$ to GUVs is shown. The mutant enzyme is derivatized with Alexa 633 (pseudocolor blue), and the more fluid domains in the membrane are stained with DiI (pseudocolor orange). Experimental conditions are as shown in Fig. 3. Images were taken at 0, 480, and 960 s after mutant enzyme addition.

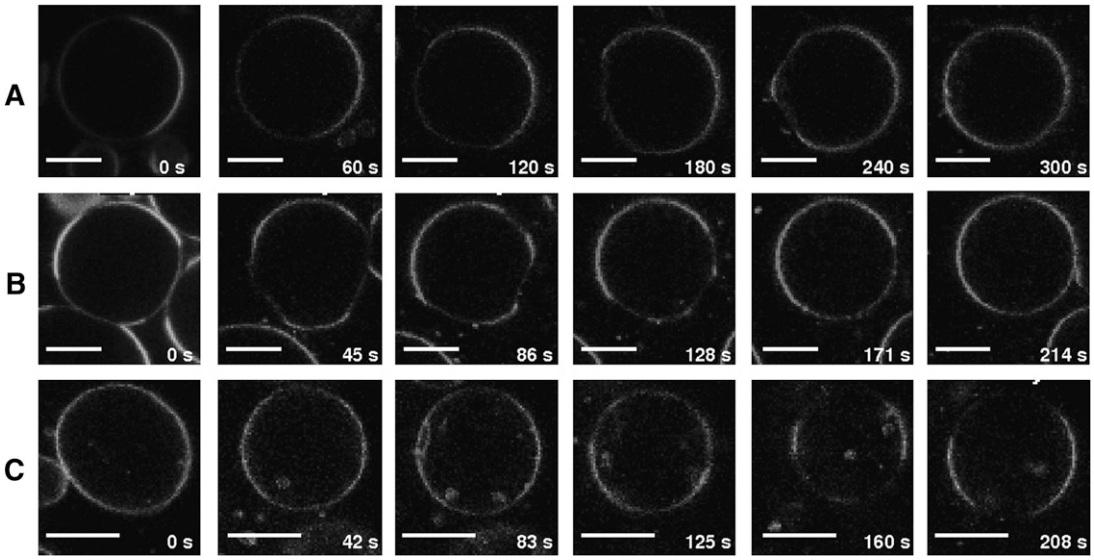

Fig. 7. Evolution of the bright (more-fluid) and dark (less-fluid) domains in GUVs is shown as a function of enzyme activity. Times after enzyme addition are given for each frame: (A) control; (B) with 10 mol% Cer; (C) with 5 mol% Cer plus 5 mol% DAG. Equatorial planes are shown. Assays were performed at 28°C. Bar = 10 μm.

Fig. SII). Alexa 633 colocalizes with DiI in all cases. The ratios of enzyme (Alexa 633) in the more-disordered region to enzyme in the less-disordered region per unit length are 2.9 ± 1.0 (control mixture) or 6.7 ± 3.9 (with 10% Cer), as estimated from experiments similar to those shown in Fig. 4. Note that rigorous calculation of this parameter would require quantitation of bright and dark areas, rather than perimeters. Only recently has a procedure allowing area measurements been published (64). However, our values can still be considered useful approximations. Also, Alexa 633 is known to exhibit a degree of self-quenching so that the actual ratios may be somewhat higher than estimated.

Effect of enzyme concentration

Enzyme concentration in the observation chamber was estimated to be about 12 μg/ml under our conditions. This value is higher than most concentrations used for PLC or sphingomyelinase assays in cuvette or in the trough of a Langmuir balance. However, it is not clear that our conditions are comparable to those used in the bulk studies, as the small thickness of our chamber (<200 μm) and the presence of the giant vesicles must decrease the enzyme diffusion due to a massive effect of unstirred layers. Generally, our observations can be considered a slow-motion version of the in vivo situation. Several experiments were performed at approximately 6 and 3 μg/ml enzyme. The same results were observed, except that reactions took longer to occur (see supplementary Fig. I).

Irreversible binding of PlcHR$_2$ to GUV bilayers

The irreversibility of PlcHR$_2$ binding to GUV bilayers was tested by incubating the vesicles with Alexa-stained enzyme for 5 min and then flushing the chamber thoroughly with buffer until the background fluorescence, corresponding to free enzyme had disappeared. The vesicle fluorescence was photographed, and the washing and photographing cycle was repeated twice more. The results (**Fig. 5**) indicate that PlcHR$_2$ binding to GUV bilayers is irreversible in the time scale of minutes. This would be compatible with the enzyme operating in the processive or "scooting mode" (65). It is interesting in this respect that Code et al. (66) have observed formation of amyloid-type fiber upon interfacial activation of PLA$_2$. This can be related to the aggregation of PLC molecules in defined patches, as proposed by Basañez et al. (61), as the required step before the burst in enzyme activity.

GUV binding of the catalytically inactive PlcHR$_2$ T178A mutant

In order to measure enzyme binding to GUV in the absence of perturbations due to the catalytic activity of PlcHR$_2$, the catalytically inactive T178A mutant was used. Alexa 633 labeling was performed as with the wild type. As shown in Fig. 1B, the mutant binds GUV in much the same way as the wild type, except that the structural changes caused by the wild-type enzyme in the bilayer (see below) are not observed with the mutant, even after long incubation times. Extensive merging of the Alexa 633 (enzyme) and DiI (disordered lipid) are observed (**Fig. 6**, bottom images), confirming the enzyme's tendency to preferentially bind domains in the liquid-disordered state.

Structural effects of PlcHR$_2$ activity

PlcHR$_2$ activity on GUV has the following main structural effects. *i*) In vesicles with coexisting liquid-ordered and liquid-disordered domains, the liquid-ordered phase shrinks and eventually disappears, and only the liquid-disordered phase prevails. *ii*) In vesicles with coexisting gel and fluid domains, the gel domains disappear at the expense of an increase in the fluid domains, and the vesicle shape evolves from a figure-8 shape to a spherical shape. *iii*) In vesicles containing 5 mol% Cer and 5 mol% DAG, homogeneous in appearance, enzyme activity generates

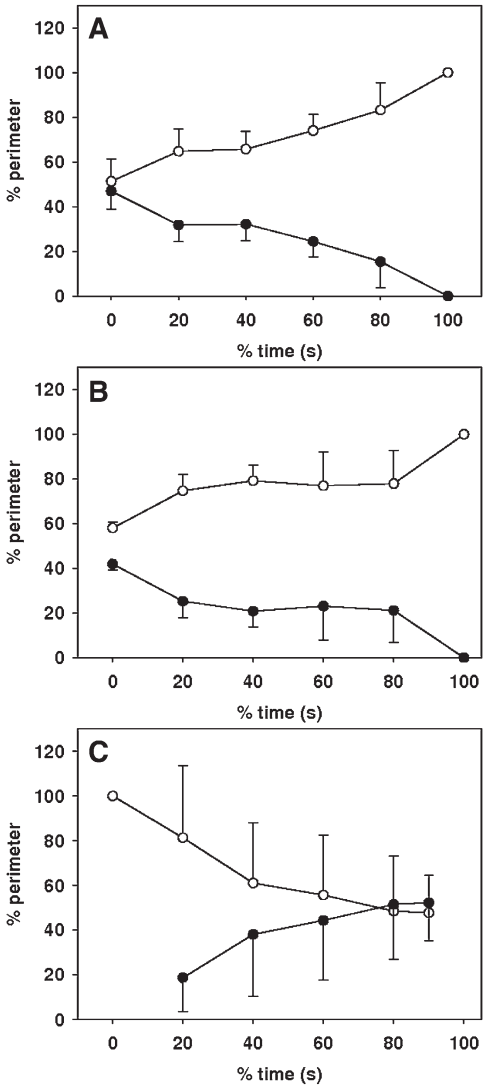

Fig. 8. Quantification of the data in vesicles was carried out as shown in Fig. 5. A: control; (B) with 10 mol% Cer; (C) with 5 mol% Cer plus 5 mol% DAG. C: Open circles indicate bright portions of the perimeters; closed circles indicate dark portions of the perimeters. Data are average values of 6–8 vesicles ± SD. Total (100%) time is 300 ± 153 s (A), 214 ± 114 s (B), and 208 ± 83 s (C).

clear separation of bright and dark domains. *iv*) In all cases, enzyme activity for prolonged times gives rise to a loss of bilayer structure, and eventually the vesicle is destroyed. This series of events, detailed below, can be seen in the supplementary material (videos).

The time sequence of $PlcHR_2$ effects on a PC:SM:PE:Ch vesicle is shown in **Fig. 7A**. DiI partitions preferentially into the more disordered domains; thus, at time 0, bright (fluid-disordered) and dark (fluid-ordered) domains coexist (23). However, over time, the bright domain(s) increases progressively, until the dark one(s) virtually disappears. Note that only the equatorial planes of vesicles are shown here. The fractions of bright and dark perimeter segments can be quantitated. Average values are shown in **Fig. 8A**. Individual variations from vesicle to vesicle exist with respect to the time required to reach the observed effects, thus the need to use normalized time scales, as shown in Fig. 7. The plotted values would parallel the progressive increase in size of the fluid-disordered domains. The overall intensity of DiI fluorescence emission per vesicle was also quantitated and found to be constant over time in the time scale of the experiments shown in Fig. 7 (data not shown). This implies that the overall vesicle structure is maintained under these conditions, when 15%–30% of PC plus SM vesicles have been hydrolyzed. The invariant overall intensity of DiI fluorescence also shows that bilayer order influences probe partition but not probe fluorescence yield.

A similar morphology is observed for enzyme-treated vesicles containing 10 mol% Cer, i.e. the bright domains increase at the expense of the dark ones (Fig. 7B). However, Cer at these concentrations is known to give rise to gel domains in bilayers (59, 60, 67–69), and Sot et al. (23) have shown that under the conditions of the present study, the dark domains seen in Fig. 7B at time 0 consist partly of liquid-ordered and partly of gel phases. Thus, in this case, a gel phase and a fluid-ordered phase are being converted into a fluid-disordered phase. Quantitative data are also very similar (Fig. 8B). Cer-containing vesicles are sometimes found to have a figure-8 (or peanut) shape (23), in which the dark domain occupies one, usually the largest, of the spherical segments. With enzyme activity, the vesicles become spherical, as shown quantitatively in **Fig. 9**. This is probably related to the morphological effects of Cer generation in GUV, as described by Devaux and coworkers (49, 70).

An interesting phenomenon is observed with vesicles containing 5 mol% Cer plus 5 mol% DAG. These vesicles are nearly homogeneous in appearance, with the occasional small dark domain (Fig. 2C). However, the enzyme activity in these vesicles gives rise to the formation of dark, gel-like or ordered domains (Figs. 7C, 8C). Rigid domain formation appears to be the result of a subtle equilibrium between the Cer tendency to lateral separation and the DAG activity toward lateral homogenization of the bilayer, both of which are modulated by the remaining lipids, PC, SM, PE, and Chol. The enzyme activity alters the compositional equilibrium by decreasing PC and SM and converting them into DAG and Cer, thus also modifying the lateral distribution of lipids in the bilayer. Fanani and Maggio (31) described the mutual modulation of sphingomyelinase and PLA_2 activities when both enzymes were added to a mixture of the corresponding substrates. Considering that $PlcHR_2$ has both sphingomyelinase and PLC activity, a similar phenomenon may be taking place here, only with one enzyme and two sets of substrates/products.

CONCLUSIONS

A system containing a complex, laterally heterogeneous lipid bilayer and an enzyme that both modifies and is influenced by the bilayer properties constitutes an attractive, although complicated, object of study. Enzyme addition generates a nonequilibrium situation in the membrane. Still, the combination of biochemical and morphological

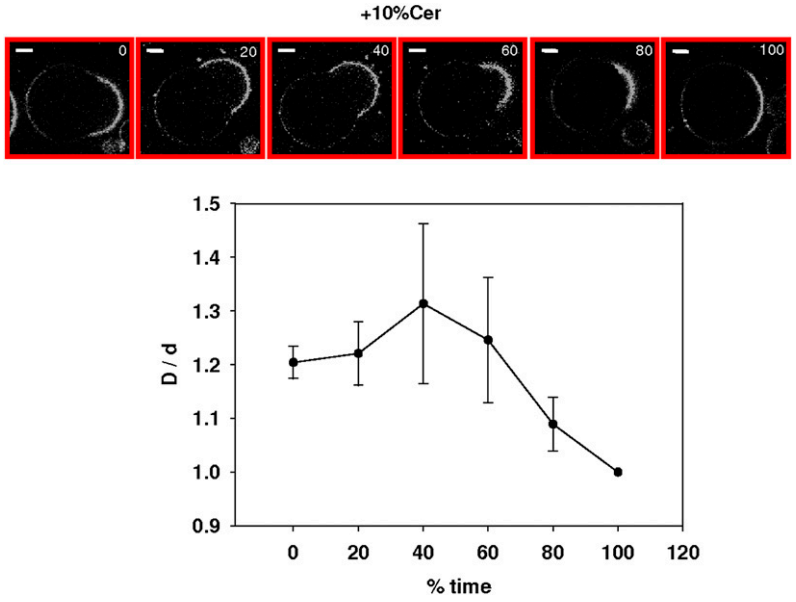

Fig. 9. Change in vesicular shape from figure-8 (or peanut) shape to spherical shape in GUVs containing 10 mol% Cer as a result of enzyme activity. D/d represents the large diameter/smaller diameter ratio, which should equal 1 for a sphere. Total (100%) time = 345 ± 100 s. The percentage of time after enzyme addition is given for each frame. Data are average values ± SD (n = 3).

techniques provides a wealth of information for the lipid-protein interactions involved. For *P. aeruginosa* $PlcHR_2$ acting on bilayers composed basically of PC, SM, PE, and Chol at equimolar ratios, the following main conclusions may be reached. *a*) Measurable enzyme binding does not occur simultaneously on all the vesicles in a preparation, even when enzyme is readily available to all of them. Rather, the phenomenon extends over a period of minutes, during which new enzyme-containing vesicles are gradually detected. Enzyme binding is initially localized to small areas from which it progresses to larger fractions of vesicle surface. *b*) The enzyme preferentially binds fluid-disordered domains over fluid-ordered or gel domains. *c*) Enzyme activity will, in most cases, fluidify or disorder the less fluid, more-ordered domains. *d*) The data are compatible with a mechanism in which enzyme binding to the bilayer is a cooperative phenomenon, and hydrolysis occurs in the "scooting mode."

The authors thank Dr. L.A. Bagatolli for help with two-photon microscopy.

REFERENCES

1. Nieva, J. L., F. M. Goñi, and A. Alonso. 1989. Liposome fusion catalytically induced by phospholipase C. *Biochemistry.* **28:** 7364–7367.
2. Luk, A. S., E. W. Kaler, and S. P. Lee. 1993. Phospholipase C-induced aggregation and fusion of cholesterol-lecithin small unilamellar vesicles. *Biochemistry.* **32:** 6965–6973.
3. Villar, A. V., A. Alonso, and F. M. Goñi. 2000. Leaky vesicle fusion induced by phosphatidylinositol-specific phospholipase C: observation of mixing of vesicular inner monolayers. *Biochemistry.* **39:** 14012–14018.
4. Villar, A. V., F. M. Goñi, and A. Alonso. 2001. Diacylglycerol effects on phosphatidylinositol-specific phospholipase C activity and vesicle fusion. *FEBS Lett.* **494:** 117–120.
5. Ruiz-Argüello, M. B., F. M. Goñi, and A. Alonso. 1998. Vesicle membrane fusion induced by the concerted activities of sphingomyelinase and phospholipase C. *J. Biol. Chem.* **273:** 22977–22982.
6. Montes, L. R., F. M. Goñi, N. C. Johnston, H. Goldfine, and A. Alonso. 2004. Membrane fusion induced by the catalytic activity of a phospholipase C/sphingomyelinase from Listeria monocytogenes. *Biochemistry.* **43:** 3688–3695.
7. Goñi, F. M., and A. Alonso. 2000. Membrane fusion induced by phospholipase C and sphingomyelinases. *Biosci. Rep.* **20:** 443–463.
8. Montes, L. R., M. Ibarguren, F. M. Goñi, M. Stonehouse, M. L. Vasil, and A. Alonso. 2007. Leakage-free membrane fusion induced by the hydrolytic activity of PlcHR(2), a novel phospholipase C/sphingomyelinase from Pseudomonas aeruginosa. *Biochim. Biophys. Acta.* **1768:** 2365–2372.
9. Stonehouse, M. J., A. Cota-Gomez, S. K. Parker, W. E. Martin, J. A. Hankin, R. C. Murphy, W. Chen, K. B. Lim, M. Hackett, A. I. Vasil, et al. 2002. A novel class of microbial phosphocholine-specific phospholipases C. *Mol. Microbiol.* **46:** 661–676.
10. Mukherjee, S., and F. R. Maxfield. 2004. Membrane domains. *Annu. Rev. Cell Dev. Biol.* **20:** 839–866.
11. Almeida, P. F., W. L. Vaz, and T. E. Thompson. 1992. Lateral diffusion and percolation in two-phase, two-component lipid bilayers. Topology of the solid-phase domains in-plane and across the lipid bilayer. *Biochemistry.* **31:** 7198–7210.
12. Bar, L. K., Y. Barenholz, and T. E. Thompson. 1997. Effect of sphingomyelin composition on the phase structure of phosphatidylcholine-sphingomyelin bilayers. *Biochemistry.* **36:** 2507–2516.
13. Holopainen, J. M., J. Y. Lehtonen, and P. K. Kinnunen. 1997. Lipid microdomains in dimyristoylphosphatidylcholine/ceramide liposomes. *Chem. Phys. Lipids.* **88:** 1–13.
14. Veiga, M. P., J. L. Arrondo, F. M. Goñi, A. Alonso, and D. Marsh. 2001. Interaction of cholesterol with sphingomyelin in mixed membranes containing phosphatidylcholine, studied by spin-label ESR and IR spectroscopies. A possible stabilization of gel-phase sphingolipid domains by cholesterol. *Biochemistry.* **40:** 2614–2622.
15. Collado, M. I., F. M. Goñi, A. Alonso, and D. Marsh. 2005. Domain formation in sphingomyelin/cholesterol mixed membranes studied by spin-label electron spin resonance spectroscopy. *Biochemistry.* **44:** 4911–4918.
16. Edidin, M. 2003. The state of lipid rafts: from model membranes to cells. *Annu. Rev. Biophys. Biomol. Struct.* **32:** 257–283.
17. Simons, K., and W. L. Vaz. 2004. Model systems, lipid rafts, and cell membranes. *Annu. Rev. Biophys. Biomol. Struct.* **33:** 269–295.
18. Goni, F. M., A. Alonso, L. A. Bagatolli, R. E. Brown, D. Marsh, M. Prieto, and J. L. Thewalt. 2008. Phase diagrams of lipid mixtures relevant to the study of membrane rafts. *Biochim. Biophys. Acta.* **1781:** 665–684.
19. Angelova, M. I., S. Soléan, P. Meléard, P. Faucon, and P. Bothorel. 1992. Preparation of giant vesicles by external AC fields. Kinetics and application. *Prog. Colloid Polym. Sci.* **89:** 127–131.
20. Montes, L. R., A. Alonso, F. M. Goñi, and L. A. Bagatolli. 2007. Giant unilamellar vesicles electroformed from native membranes and organic lipid mixtures under physiological conditions. *Biophys. J.* **93:** 3548–3554.

21. Bagatolli, L. A., S. A. Sanchez, T. Hazlett, and E. Gratton. 2003. Giant vesicles, Laurdan, and two-photon fluorescence microscopy: evidence of lipid lateral separation in bilayers. *Methods Enzymol.* **360:** 481–500.
22. Bagatolli, L. A., J. H. Ipsen, A. C. Simonsen, and O. G. Mouritsen. 2010. An outlook on organization of lipids in membranes: searching for a realistic connection with the organization of biological membranes. *Prog. Lipid Res.* **49:** 378–389.
23. Sot, J., M. Ibarguren, J. V. Busto, L. R. Montes, F. M. Goñi, and A. Alonso. 2008. Cholesterol displacement by ceramide in sphingomyelin-containing liquid-ordered domains, and generation of gel regions in giant lipidic vesicles. *FEBS Lett.* **582:** 3230–3236.
24. Chiantia, S., N. Kahya, J. Ries, and P. Schwille. 2006. Effects of ceramide on liquid-ordered domains investigated by simultaneous AFM and FCS. *Biophys. J.* **90:** 4500–4508.
25. Megha, P. Sawatzki, T. Kolter, R. Bittman, and E. London. 2007. Effect of ceramide N-acyl chain and polar headgroup structure on the properties of ordered lipid domains (lipid rafts). *Biochim. Biophys. Acta.* **1768:** 2205–2212.
26. Taniguchi, Y., T. Ohba, H. Miyata, and K. Ohki. 2006. Rapid phase change of lipid microdomains in giant vesicles induced by conversion of sphingomyelin to ceramide. *Biochim. Biophys. Acta.* **1758:** 145–153.
27. Bianco, I. D., G. D. Fidelio, and B. Maggio. 1989. Modulation of phospholipase A2 activity by neutral and anionic glycosphingolipids in monolayers. *Biochem. J.* **258:** 95–99.
28. Bianco, I. D., G. D. Fidelio, R. K. Yu, and B. Maggio. 1991. Degradation of dilauroylphosphatidylcholine by phospholipase A2 in monolayers containing glycosphingolipids. *Biochemistry.* **30:** 1709–1714.
29. Maggio, B., I. D. Bianco, G. G. Montich, G. D. Fidelio, and R. K. Yu. 1994. Regulation by gangliosides and sulfatides of phospholipase A2 activity against dipalmitoyl- and dilauroylphosphatidylcholine in small unilamellar bilayer vesicles and mixed monolayers. *Biochim. Biophys. Acta.* **1190:** 137–148.
30. Daniele, J. J., B. Maggio, I. D. Bianco, F. M. Goni, A. Alonso, and G. D. Fidelio. 1996. Inhibition by gangliosides of *Bacillus cereus* phospholipase C activity against monolayers, micelles and bilayer vesicles. *Eur. J. Biochem.* **239:** 105–110.
31. Fanani, M. L., and B. Maggio. 1997. Mutual modulation of sphingomyelinase and phospholipase A2 activities against mixed lipid monolayers by their lipid intermediates and glycosphingolipids. *Mol. Membr. Biol.* **14:** 25–29.
32. Jungner, M., H. Ohvo, and J. P. Slotte. 1997. Interfacial regulation of bacterial sphingomyelinase activity. *Biochim. Biophys. Acta.* **1344:** 230–240.
33. Nieva, J. L., A. Alonso, G. Basanez, F. M. Goni, A. Gulik, R. Vargas, and V. Luzzati. 1995. Topological properties of two cubic phases of a phospholipid:cholesterol:diacylglycerol aqueous system and their possible implications in the phospholipase C-induced liposome fusion. *FEBS Lett.* **368:** 143–147.
34. Ahyayauch, H., A. V. Villar, A. Alonso, and F. M. Goñi. 2005. Modulation of PI-specific phospholipase C by membrane curvature and molecular order. *Biochemistry.* **44:** 11592–11600.
35. Bailey, R. W., E. D. Olson, M. P. Vu, T. J. Brueseke, L. Robertson, R. E. Christensen, K. H. Parker, A. M. Judd, and J. D. Bell. 2007. Relationship between membrane physical properties and secretory phospholipase A2 hydrolysis kinetics in S49 cells during ionophore-induced apoptosis. *Biophys. J.* **93:** 2350–2362.
36. Vest, R., R. Wallis, L. B. Jensen, A. C. Haws, J. Callister, B. Brimhall, A. M. Judd, and J. D. Bell. 2006. Use of steady-state laurdan fluorescence to detect changes in liquid ordered phases in human erythrocyte membranes. *J. Membr. Biol.* **211:** 15–25.
37. Davidsen, J., K. Jorgensen, T. L. Andresen, and O. G. Mouritsen. 2003. Secreted phospholipase A(2) as a new enzymatic trigger mechanism for localised liposomal drug release and absorption in diseased tissue. *Biochim. Biophys. Acta.* **1609:** 95–101.
38. Leidy, C., L. Linderoth, T. L. Andresen, O. G. Mouritsen, K. Jorgensen, and G. H. Peters. 2006. Domain-induced activation of human phospholipase A2 type IIA: local versus global lipid composition. *Biophys. J.* **90:** 3165–3175.
39. Holopainen, J. M., M. Subramanian, and P. K. Kinnunen. 1998. Sphingomyelinase induces lipid microdomain formation in a fluid phosphatidylcholine/sphingomyelin membrane. *Biochemistry.* **37:** 17562–17570.
40. Contreras, F. X., J. Sot, M. B. Ruiz-Arguello, A. Alonso, and F. M. Goñi. 2004. Cholesterol modulation of sphingomyelinase activity at physiological temperatures. *Chem. Phys. Lipids.* **130:** 127–134.
41. Simonsen, A. C., U. B. Jensen, and P. L. Hansen. 2006. Hydrolysis of fluid supported membrane islands by phospholipase A(2): time-lapse imaging and kinetic analysis. *J. Colloid Interface Sci.* **301:** 107–115.
42. De Tullio, L., B. Maggio, and M. L. Fanani. 2008. Sphingomyelinase acts by an area-activated mechanism on the liquid-expanded phase of sphingomyelin monolayers. *J. Lipid Res.* **49:** 2347–2355.
43. Fanani, M. L., L. De Tullio, S. Hartel, J. Jara, and B. Maggio. 2008. Sphingomyelinase-induced domain shape relaxation driven by out-of-equilibrium changes of composition. *Biophys. J.* **96:** 67–76.
44. Silva, L. C., A. H. Futerman, and M. Prieto. 2009. Lipid raft composition modulates sphingomyelinase activity and ceramide-induced membrane physical alterations. *Biophys. J.* **96:** 3210–3222.
45. Wick, R., and P. L. Luisi. 1996. Enzyme-containing liposomes can endogenously produce membrane-constituting lipids. *Chem. Biol.* **3:** 277–285.
46. Sanchez, S. A., L. A. Bagatolli, E. Gratton, and T. L. Hazlett. 2002. A two-photon view of an enzyme at work: *Crotalus atrox* venom PLA2 interaction with single-lipid and mixed-lipid giant unilamellar vesicles. *Biophys. J.* **82:** 2232–2243.
47. Holopainen, J. M., M. I. Angelova, and P. K. Kinnunen. 2000. Vectorial budding of vesicles by asymmetrical enzymatic formation of ceramide in giant liposomes. *Biophys. J.* **78:** 830–838.
48. Holopainen, J. M., M. I. Angelova, T. Soderlund, and P. K. Kinnunen. 2002. Macroscopic consequences of the action of phospholipase C on giant unilamellar liposomes. *Biophys. J.* **83:** 932–943.
49. Lopez-Montero, I., M. Velez, and P. F. Devaux. 2007. Surface tension induced by sphingomyelin to ceramide conversion in lipid membranes. *Biochim. Biophys. Acta.* **1768:** 553–561.
50. Ibarguren, M., P. H. Bomans, P. M. Frederik, M. Stonehouse, A. I. Vasil, M. L. Vasil, A. Alonso, and F. M. Goni. 2010. End-products diacylglycerol and ceramide modulate membrane fusion induced by a phospholipase C/sphingomyelinase from Pseudomonas aeruginosa. *Biochim. Biophys. Acta.* **1798:** 59–64.
51. Vasil, M. L., M. J. Stonehouse, A. I. Vasil, S. J. Wadsworth, H. Goldfine, R. E. Bolcome III, and J. Chan. 2009. A complex extracellular sphingomyelinase of Pseudomonas aeruginosa inhibits angiogenesis by selective cytotoxicity to endothelial cells. *PLoS Pathog.* **5:** e1000420.
52. Felts, R. L., T. J. Reilly, and J. J. Tanner. 2006. Structure of Francisella tularensis AcpA: prototype of a unique superfamily of acid phosphatases and phospholipases C. *J. Biol. Chem.* **281:** 30289–30298.
53. Fidorra, M., L. Duelund, C. Leidy, A. C. Simonsen, and L. A. Bagatolli. 2006. Absence of fluid-ordered/fluid-disordered phase coexistence in ceramide/POPC mixtures containing cholesterol. *Biophys. J.* **90:** 4437–4451.
54. Ruiz-Argüello, M. B., G. Basáñez, F. M. Goñi, and A. Alonso. 1996. Different effects of enzyme-generated ceramides and diacylglycerols in phospholipid membrane fusion and leakage. *J. Biol. Chem.* **271:** 26616–26621.
55. López, D. J. 2008. Actividades esfingomielinasa bacterianas y de mamíferos. Caracterización y efectos estructurales en membranas. PhD thesis. University of the Basque Country, Bilbao, Spain.
56. Quinn, P. J., and C. Wolf. 2009. Hydrocarbon chains dominate coupling and phase coexistence in bilayers of natural phosphatidylcholines and sphingomyelins. *Biochim. Biophys. Acta.* **1788:** 1126–1137.
57. Basáñez, G., G. D. Fidelio, F. M. Goni, B. Maggio, and A. Alonso. 1996. Dual inhibitory effect of gangliosides on phospholipase C-promoted fusion of lipidic vesicles. *Biochemistry.* **35:** 7506–7513.
58. Flores-Diaz, M., A. Alape-Giron, G. Clark, B. Catimel, Y. Hirabayashi, E. Nice, J. M. Gutierrez, R. Titball, and M. Thelestam. 2005. A cellular deficiency of gangliosides causes hypersensitivity to Clostridium perfringens phospholipase C. *J. Biol. Chem.* **280:** 26680–26689.
59. Staneva, G., C. Chachaty, C. Wolf, K. Koumanov, and P. J. Quinn. 2008. The role of sphingomyelin in regulating phase coexistence in complex lipid model membranes: competition between ceramide and cholesterol. *Biochim. Biophys. Acta.* **1778:** 2727–2739.
60. Staneva, G., A. Momchilova, C. Wolf, P. J. Quinn, and K. Koumanov. 2009. Membrane microdomains: role of ceramides in the maintenance of their structure and functions. *Biochim. Biophys. Acta.* **1788:** 666–675.
61. Basáñez, G., J. L. Nieva, F. M. Goni, and A. Alonso. 1996. Origin of the lag period in the phospholipase C cleavage of phospholipids in membranes. Concomitant vesicle aggregation and enzyme activation. *Biochemistry.* **35:** 15183–15187.
62. Fanani, M. L., and B. Maggio. 2000. Kinetic steps for the hydrolysis of sphingomyelin by Bacillus cereus sphingomyelinase in lipid monolayers. *J. Lipid Res.* **41:** 1832–1840.

63. Bagatolli, L. A. 2006. To see or not to see: lateral organization of biological membranes and fluorescence microscopy. *Biochim. Biophys. Acta.* **1758:** 1541–1556.
64. Fidorra, M., A. Garcia, J. H. Ipsen, S. Hartel, and L. A. Bagatolli. 2009. Lipid domains in giant unilamellar vesicles and their correspondence with equilibrium thermodynamic phases: a quantitative fluorescence microscopy imaging approach. *Biochim. Biophys. Acta.* **1788:** 2142–2149.
65. Jain, M. K., J. Rogers, J. F. Marecek, F. Ramirez, and H. Eibl. 1986. Effect of the structure of phospholipid on the kinetics of intravesicle scooting of phospholipase A2. *Biochim. Biophys. Acta.* **860:** 462–474.
66. Code, C., Y. Domanos, A. Jutila, and P. K. Kinnunen. 2008. Amyloid-type fiber formation in control of enzyme action: interfacial activation of phospholipase A_2. *Biophys. J.* **95:** 215–224.
67. Veiga, M. P., J. L. Arrondo, F. M. Goñi, and A. Alonso. 1999. Ceramides in phospholipid membranes: effects on bilayer stability and transition to nonlamellar phases. *Biophys. J.* **76:** 342–350.
68. Carrer, D. C., and B. Maggio. 1999. Phase behavior and molecular interactions in mixtures of ceramide with dipalmitoylphosphatidylcholine. *J. Lipid Res.* **40:** 1978–1989.
69. Goni, F. M., and A. Alonso. 2009. Effects of ceramide and other simple sphingolipids on membrane lateral structure. *Biochim. Biophys. Acta.* **1788:** 169–177.
70. Lopez-Montero, I., N. Rodriguez, S. Cribier, A. Pohl, M. Velez, and P. F. Devaux. 2005. Rapid transbilayer movement of ceramides in phospholipid vesicles and in human erythrocytes. *J. Biol. Chem.* **280:** 25811–25819.